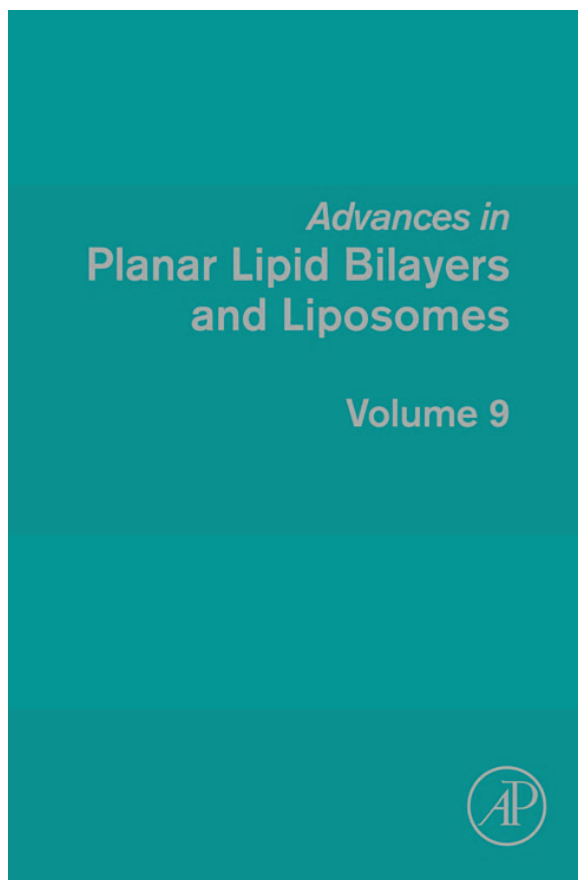


**Provided for non-commercial research and educational use only.
Not for reproduction, distribution or commercial use.**

This chapter was originally published in the book *Advances in Planar Lipid Bilayers and Liposomes*, Vol. 9, published by Elsevier, and the attached copy is provided by Elsevier for the author's benefit and for the benefit of the author's institution, for non-commercial research and educational use including without limitation use in instruction at your institution, sending it to specific colleagues who know you, and providing a copy to your institution's administrator.



All other uses, reproduction and distribution, including without limitation commercial reprints, selling or licensing copies or access, or posting on open internet sites, your personal or institution's website or repository, are prohibited. For exceptions, permission may be sought for such use through Elsevier's permissions site at:

<http://www.elsevier.com/locate/permissionusematerial>

From: Šárka Perutková, Matej Daniel, Gregor Dolinar, Michael Rappolt, Veronika Kralj-Iglič, and Aleš Iglič, Stability of the Inverted Hexagonal Phase. In A. Leitmannova Liu and H.T. Tien, editors: *Advances in Planar Lipid Bilayers and Liposomes*, Vol. 9, Burlington: Academic Press, 2009, pp. 237-278.

ISBN: 978-0-12-374822-5

© Copyright 2009 Elsevier Inc.

Academic Press.

STABILITY OF THE INVERTED HEXAGONAL PHASE

Šárka Perutková,^{1,*} Matej Daniel,² Gregor Dolinar,³
Michael Rappolt,⁴ Veronika Kralj-Iglič,⁵ and Aleš Iglič¹

Contents

1. Introduction	238
1.1. Mathematical Description of Membrane Curvature	240
1.2. Influence of Spontaneous Curvature on the Self-Assembling Process	242
2. Inverted Hexagonal Phase	244
2.1. Relevance of Nonlamellar Phases in Biological Systems	244
2.2. Geometry of the Inverted Hexagonal Phase	244
2.3. Models of the Transition of the Lamellar to Inverted Hexagonal Phase	246
2.4. Models of Free Energy of the Inverted Hexagonal Phase	248
3. Free Energy of Lipid Monolayers	252
3.1. Bending Energy of Lipid Monolayers	252
3.2. Interstitial Energy of the Inverted Hexagonal Phase	258
3.3. Total Free Energy per Lipid Molecule	260
4. Estimation of Model Constants	261
5. Determination of Equilibrium Configuration of Planar and Inverted Cylindrical Systems	262
5.1. Numerical Solution	262
5.2. Results of Equilibrium Configurations of Planar and Inverted Cylindrical Systems	262
5.3. Influence of the Direct Interaction Constant \tilde{k}	267

* Corresponding author. Tel.: +386 31 356 953; Fax: +386 1 4768 850;
E-mail address: sarka.perutkova@fe.uni-lj.si

¹ Laboratory of Biophysics, Faculty of Electrical Engineering, University of Ljubljana, Slovenia

² Laboratory of Biomechanics, Faculty of Mechanical Engineering, Czech Technical University in Prague, Czech Republic

³ Laboratory of Mathematics, Faculty of Electrical Engineering, University of Ljubljana, Slovenia

⁴ Institute of Biophysics and Nanosystems Research, Austrian Academy of Sciences c/o Sincrotrone Trieste, Italy

⁵ Laboratory of Clinical Biophysics, Faculty of Medicine, University of Ljubljana, Slovenia

6. Lamellar to Inverted Hexagonal Phase Transition	267
6.1. Determination of Pivotal Map of Nucleation Contour by Minimization of Monolayer Bending Energy	267
6.2. Determination of Equilibrium Configuration of Lamellar to Inverted Hexagonal Phase Transition by Monte Carlo Simulated Annealing Method	270
6.3. Results: Equilibrium Configuration of Nucleation of the Lamellar to Inverted Hexagonal Phase Transition	271
7. Discussion and Conclusions	274
Acknowledgments	275
References	275

Abstract

The inverted hexagonal phase (H_{II}) belongs to the biologically most significant nonlamellar lipid phases in biomembranes. Hence the geometric properties and conditions of transition to the H_{II} phase are nowadays widely studied. In this chapter we offer a brief overview on the mechanics of the H_{II} lipid phase. In our derivation of the free energy of lipid monolayers, we assume that lipid molecules are in general anisotropic with respect to the axis perpendicular to the membrane plane. In our model the expression for the lipid monolayer free energy consists of two energy contributions: the bending energy which involves also a deviatoric term, and the interstitial energy which describes the deformation energy due to stretching of the phospholipid molecule chains. On the basis of the derived expression for the lipid monolayer free energy, we theoretically predict optimal geometry and physical conditions for the stability of the inverted hexagonal phase. Using the Monte Carlo simulated annealing method, we theoretically describe first steps in the L_α - H_{II} phase transition, which may contribute to a better understanding of different biologically important processes within biomembranes.

1. INTRODUCTION

One of the main components of biological membranes are phospholipids. They have amphiphatic character, that is, they comprise a polar headgroup as well as nonpolar hydrocarbon chains in one molecule. Such molecules in aqueous solution undergo a self-assembling process and form various structures. Biologically important lipid/water systems are known for their rich polymorphism [1]. Driving force of this process is predominantly the hydrophobic effect where the hydrophilic (polar) surfaces are in contact with aqueous solution while the hydrophobic (nonpolar) parts composed of hydrocarbon chains are hidden from water [2, 3]. The most common and biologically most relevant phase is the fluid lamellar lipid bilayer

phase (L_{α}). The bilayer of lipid molecules represents the basic building block of the plasma membrane, which encloses the cell interior. Nevertheless, nonlamellar model membranes are subject of increasing interest [1, 4–6], due to their importance in living organisms and due to their promising technical applications such as in drug delivery [7, 8], gene transport and nanotechnology [9].

The curvature of different monolayer and bilayer lipid structures (Fig. 1) depends to a great extent on the intrinsic shape of the phospholipid molecules, which in turn depends on the temperature, degree of hydration, presence of specific enzymes, pH, etc. [10].

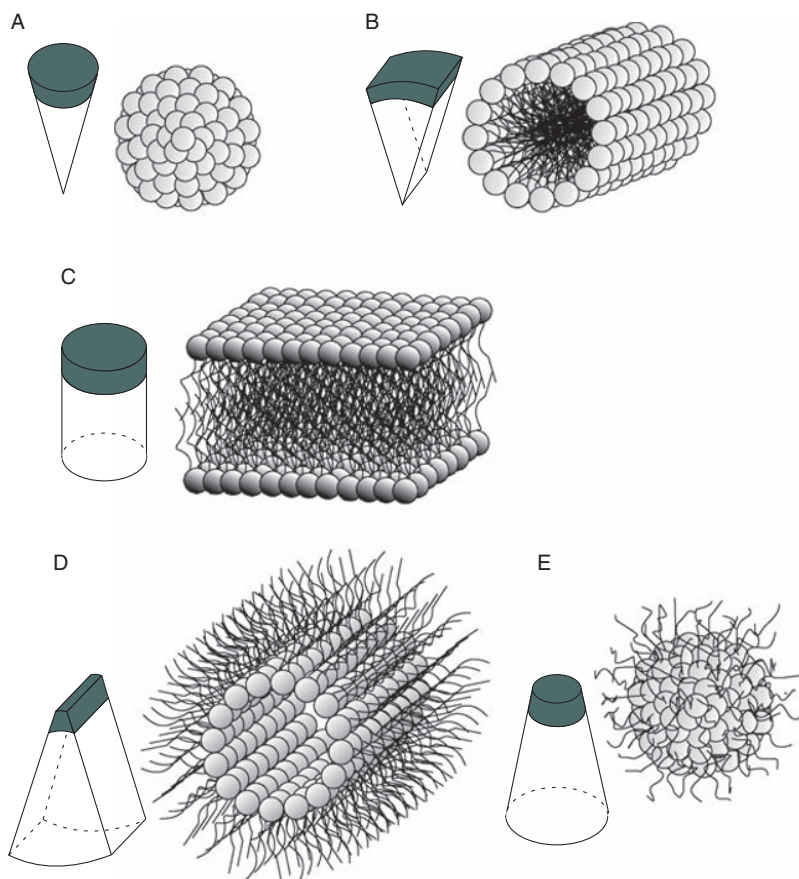


Figure 1 Schematically depicted polymorphism of phospholipid aggregates. Aggregated forms with appropriate shapes of phospholipid molecules: (A) spherical micelle, (B) cylinder, (C) bilayer, (D) inverted cylinder, and (E) inverted micelle.

Flat lipid bilayers are formed preferentially, when the lipid molecules have cylindrical shapes (Fig. 1C), whereas cylindrical monolayers are formed when the lipid molecules are wedge shaped (as depicted in Fig. 1B and D). Conical and inverted conical shapes of lipids favor spherical (Fig. 1A) and inverted spherical (Fig. 1E) micellar shapes, respectively (see also Ref. [11]).

1.1. Mathematical Description of Membrane Curvature

Biological membranes may be in the first approximation considered as curved and deformable smooth plates that are described by two principal radii (curvatures) at each point of the surface. Consider for the moment the phospholipid monolayer as a pure mathematical surface. At every point P on this surface one can find a vector normal to the surface and the corresponding normal plane which contains the normal vector (Fig. 2). There is an infinite number of such normal planes, but only two orthogonal normal planes contain curves of intersection with maximum and minimum curvature (see Fig. 2). These two curvatures are named the two principal curvatures of the surface at the given point P and are defined as [1]

$$C_1 = \frac{1}{r_1} \quad \text{and} \quad C_2 = \frac{1}{r_2} \quad (1)$$

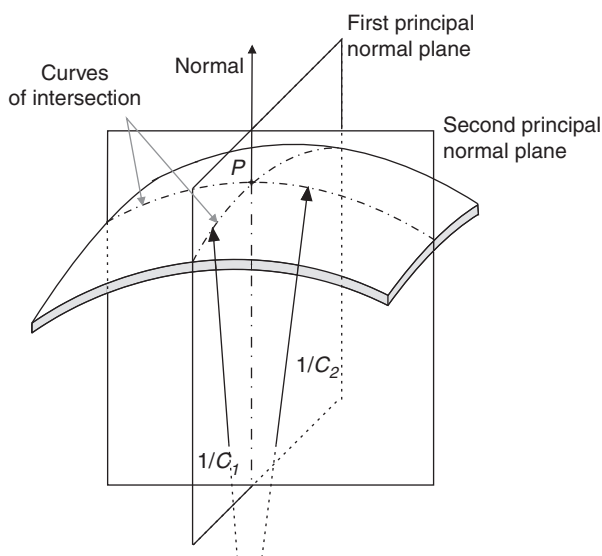


Figure 2 A schematic figure of the phospholipid monolayer. In the point P the normal surface is shown together with a pair of orthogonal principal planes that define the two principal curvatures C_1 and C_2 .

For the sake of later computations, the principal curvatures are written in a tensor notation as a diagonalized curvature tensor:

$$\underline{C} = \begin{bmatrix} C_1 & 0 \\ 0 & C_2 \end{bmatrix} \quad (2)$$

Within the theory of elasticity, the membrane curvature at a given point is usually described by the mean and the Gaussian curvature, that are invariants of the curvature tensor \underline{C} (Eq. (2)). The mean curvature H is related to the trace of the curvature tensor \underline{C} and the Gaussian curvature K is the determinant of \underline{C} [1]:

$$H = \frac{C_1 + C_2}{2} \quad (3)$$

$$K = C_1 C_2 \quad (4)$$

For the lipid monolayer of finite thickness, the following convention was adopted [1]: when, for instance, the pivotal plane (molecular area in pivotal plane does not change upon bending deformation [12]) bends toward the chain region, we define the curvature positive ($C > 0$), whereas when the pivotal plane bends toward the water region the curvature is negative ($C < 0$) (Fig. 3). According to this convention the mean curvature H (Eq. (3)) can be positive or negative, that is, the monolayer can be regular or inverted. For positive values of K the planes are naturally convex or concave and bend round to form closed shells, micelles or inverted micelles, respectively. On the other hand, when K is negative the principal curvatures are of opposite sign, that is, the plane is saddle-like [1].

For planar and spherical surfaces the principal curvatures are equal while for saddle-like and cylindrical planes the principal curvatures are different. High anisotropy in the curvature (a large difference between the two

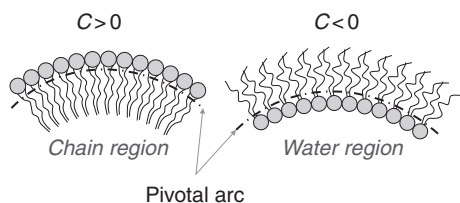


Figure 3 Sign convention of the curvature $C = C_1 \cos^2 \beta + C_2 \sin^2 \beta$ of the normal cut of the lipid monolayer. The curvature C is positive when the monolayer is bent toward the chain region and negative when the monolayer is bent toward the water region. The angle β describes the orientation of the normal plane with respect to the first principal normal plane.

principal curvatures) has been revealed in numerous membrane systems, for example, in phospholipid bilayer nanotubes [13–16], torocytic endovesicles of erythrocyte membranes [17, 18], phospholipid bilayer membrane pores [19, 20] and narrow necks of phospholipid bilayers connecting buds to the mother membrane [21]. To explain the stability of these structures instead of the Gaussian curvature another invariant is advantageous in description of membrane free (elastic) energy, namely the curvature deviator D [21]:

$$D = \frac{|C_1 - C_2|}{2} \quad (5)$$

The invariants H , K , and D are connected through the relation:

$$H^2 = D^2 + K \quad (6)$$

1.2. Influence of Spontaneous Curvature on the Self-Assembling Process

Obviously the curvature of membranes depends on the intrinsic shape of the phospholipid molecules (see Fig. 1). Hence noncylindrically shaped phospholipids self-assemble in aqueous solutions in nonplanar structures. The tendency to curve the shape of the monolayer without any external torques and forces is called the spontaneous (intrinsic) curvature [10]. The definition of the principal intrinsic curvatures that define the intrinsic shape of the lipid molecules (see Fig. 4) is very similar to the description of membrane curvature. The principal intrinsic curvatures are defined as [22, 23]:

$$C_{1m} = \frac{1}{r_{m1}} \quad (7)$$

and

$$C_{2m} = \frac{1}{r_{m2}} \quad (8)$$

where r_{m1} and r_{m2} are the principal radii of a monolayer that would completely suit the shape of the molecule. Written in tensor notation:

$$\underline{C}_m = \begin{bmatrix} C_{1m} & 0 \\ 0 & C_{2m} \end{bmatrix} \quad (9)$$

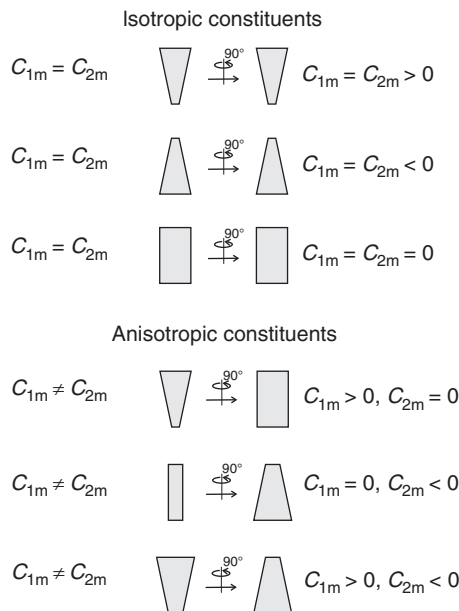


Figure 4 Molecular sketches describing differences between isotropic and anisotropic phospholipid molecules and values of their principal intrinsic curvatures.

where \underline{C}_m is defined as an intrinsic curvature tensor [21, 23].

Similar to the mean curvature H , we can define the mean intrinsic curvature H_m , which is now related to the molecular shape:

$$H_m = \frac{C_{1m} + C_{2m}}{2} \quad (10)$$

and intrinsic curvature deviator of the molecule:

$$D_m = \frac{|C_{1m} - C_{2m}|}{2} \quad (11)$$

If the intrinsic principal curvatures are different ($C_{1m} \neq C_{2m}$), the molecules are anisotropic. If the intrinsic curvatures are equal ($C_{1m} = C_{2m}$), the membrane constituents are isotropic (Fig. 4). Isotropic constituents with zero intrinsic curvatures ($C_{1m} = C_{2m} = 0$) will tend to form planar monolayers, while the constituents having inverted conical shape ($C_{1m} = 0, C_{2m} < 0$) will favor the formation of an inverted hexagonal structure [11] (see also Fig. 1). The intrinsic principal curvatures account for the geometrical

shape of the lipid molecule and the local interactions of the molecule with its surroundings, including the hydration effects [24].

2. INVERTED HEXAGONAL PHASE

The inverted hexagonal phase (H_{II}) is one of the lipid mesophases that are important for many biological processes in nature. Understanding the mechanisms of their formation and stability, and their physical properties may help us to elucidate their biological functions.

2.1. Relevance of Nonlamellar Phases in Biological Systems

The bicontinuous cubic phase, inverse hexagonal phase, and inverse micellar cubic phase belong to the biologically most relevant nonlamellar mesophases. These mesophases resist excess of water and thus they are stable under certain conditions in biological systems [6, 25].

It is known that a wide range of phospholipids which occur in biological organisms may self-assemble into nonlamellar structures when they are extracted from cells and rehydrated in aqueous solution. However, despite the fact that many nonlamellar phases have been undoubtedly identified also in various biological systems [26], still little is understood concerning their function. The induction of nonplanar mesophases might play a role in the regulation of protein function, further, membrane fusion for instance in endo- and exocytosis is thought to be dependent on such highly curved lipid structures. It is also supposed that interbilayer tight junctions host nonbilayer structures. Direct evidence for the formation of the stable H_{II} phase was found in paracrystalline inclusions of the retina [27].

The nonlamellar structures of phospholipids are also common in some species of bacteria. It was suggested that the bilayers of bacteria are close to the transition from lamellar to nonlamellar structure [10]. Many different types of bacteria can enzymatically change the intrinsic curvature of phospholipids, consequently, they can prefer the nonlamellar phases [10].

2.2. Geometry of the Inverted Hexagonal Phase

The lipids in the inverted hexagonal phase are self-assembled in long tubes arranged in a hexagonal lattice. Figures 5 and 6 show the geometry of the H_{II} phase: two neighboring tubes with diameter r are located at the distance a . The phospholipid chains point outward from the cylinder surface defined as the pivotal plane while the headgroups form polar nanotubes filled with aqueous solution. Experiments revealed high anisotropy in the curvature (one principal curvature is equal to negative inverse value of radius of the tube and the second principal curvature is equal to zero) of tubes of the H_{II} phase.

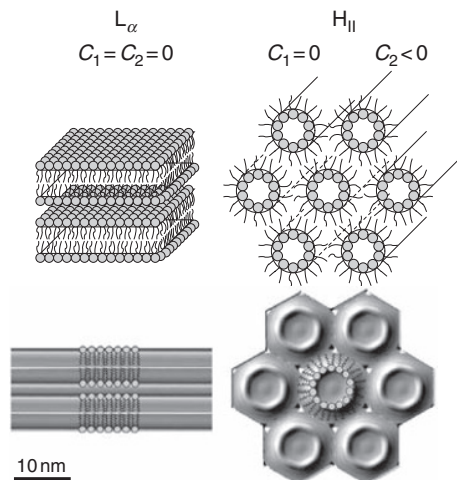


Figure 5 A scheme and a corresponding electron density map of the lamellar fluid (L_{α}) phase (left) and of the inverted hexagonal (H_{II}) phase (right). The configurations of the lipid molecules are indicated. In the L_{α} phase both principal curvatures are equal to zero, while in the H_{II} phase one of the principal curvatures is equal to zero and the other one is negative. The data for the electron density reconstructions are taken from Ref. [28]. The maps depict the POPE/water structures at the phase transition temperature of 74 °C (compare also Table 1). Adapted from Ref. [29].

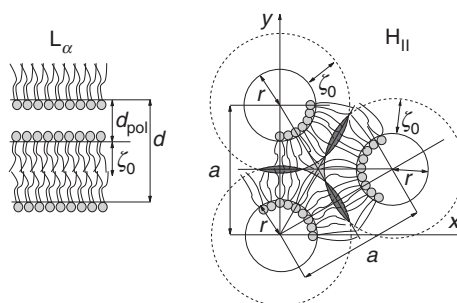


Figure 6 Geometry of the lamellar and inverted hexagonal phases. One bilayer and one neighboring monolayer are depicted for the lamellar phase. The lattice unit of lamellar phase (d -spacing) (d) and distance of polar region between the two bilayers (d_{pol}) are denoted. For the inverted hexagonal phase three cylinders of radius r at the distance a are depicted. ζ_0 denotes the equilibrium length of hydrocarbon chains. The H_{II} phase requires stretching or compressing of some of the hydrocarbon chains as shown schematically. Adapted from Ref. [29].

It can be seen in Fig. 6 that not all lipid tails in the hexagonal lattice have the same length. There are triangular regions (called voids) between neighboring tubes that are considerably energetically expensive, because the lipid chains in these regions need to stretch beyond the average length ζ_0 . In theoretical studies of stability of inverted hexagonal phases, it is therefore necessary to take into account an energy term which accounts for the stretching of the hydrocarbon chains in the void regions [24, 30–32].

Some recent studies have shown that the cross sections of the tubes in the inverted hexagonal phase is not precisely circular but it is rather an intermediate between a circle and a hexagon [31, 33]. In our case we suppose, for sake of simplicity, that the cross section is circular.

2.3. Models of the Transition of the Lamellar to Inverted Hexagonal Phase

Transitions between different phospholipid phases and mechanisms that drive these transitions are of special interest. To interpret the experimental data and to contribute to a better understanding of underlying mechanisms, different models have been put forward [24, 28, 30, 34, 35].

The majority of models of the formation of the inverted hexagonal phase have in common the assumption that nucleation starts with a linearly localized lipid rearrangement. Based on freeze–fracture electron microscopy experiments, a deformation pair of intramembrane cylinders embedded in a tight junction was proposed [35], and also monolayer embedded lipid tubes forming via the coalescence of a “pearl string” of inverted micellar intermediates (IMIs) was suggested by Hui *et al.* [36]. In 1986 Siegel further elaborated this model of the L_α – H_{II} transition [30]. He proposed a three-step process with forming of intermediates driven by changes in temperature and lipid composition. The first step is formation of IMIs, which forms between two sufficiently close apposed bilayers. The IMI can diffuse within the plane of the membrane and form IMI coalescence representing the second step. Two possible ways of IMI coalescence were suggested. Two spherical micelles can fuse into a single rod shaped micelle and form rod micellar intermediates (RMIs) or they can separate within the coalescence intermediate and form line defects (LDs) [30].

Based on the temperature–dependent experimental results from differential scanning calorimetry and small–angle X–ray scattering, a similar view on L_α – H_{II} transition is given by Rappolt *et al.* [28, 34]. The hypothesis of the growth mechanism of the first few rods is connected with spontaneous creation of the line defect (water core) at the transition temperature. The first rod is created due to the spontaneous monolayer curvature, which induces the formation of new water cores. The pivotal plane arrangement corresponding to the first few steps of transition was proposed in Ref. [34] (see Figs. 7 and 8). The first cylinder of the H_{II} phase forms from the linearly

localized lipid rearrangement between two bilayers. Thus, a system of one cylinder, two monolayers, and bulby closures on both sides of the cylinder originates. The bulby closures are created from neighboring disjunct layers as a consequence of reducing void apolar regions. The two outer monolayer leaflets follow the contours of the cylinder and the bulby closures. This configuration is the smallest unit to study the nucleation of the H_{II} - L_{α} transition (Fig. 7).

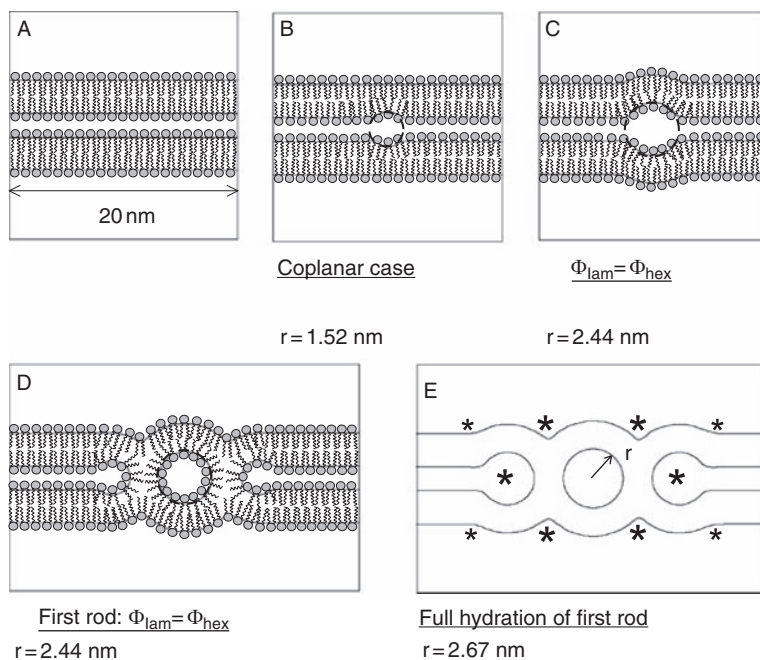


Figure 7 Intermediate steps in the formation of a cylinder between two bilayers. The structural schemes base on structural data of POPE recorded at the transition temperature $T = 74$ °C [28]. Pivotal interfaces are outlined with full lines and for the ease of interpretation lipid molecules are superimposed in the first four panels. (A) The fluid lamellar phase can be decomposed into steric monolayer thickness (2.27 nm) and free water layer thickness per lipid molecule (0.27 nm). (B) Allowing for spontaneous splay of lipid molecules a line defect may form, which is integrated in the stack of bilayers in a coplanar fashion. (C) If one sets the water concentration per lipid in the line defect, Φ_{hex} , to be equal to the water concentration given in the fluid lamellar phase, Φ_{lam} , then the radius of the pivotal plane increases from $r = 1.52$ to 2.44 nm. (D) This panel shows the formation of a first rod under the condition of $\Phi_{\text{lam}} = \Phi_{\text{hex}}$. (E) Finally, full hydration of the first cylinder in between of two bilayers increases the pivotal plane radius to $r = 2.67$ nm. Loci for the formation of new cylinders are marked with stars. Sketches are adapted from Ref. [34].

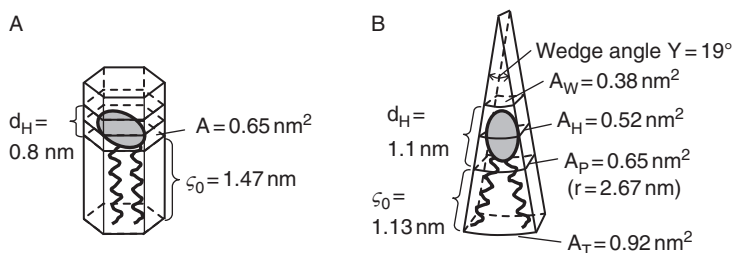


Figure 8 Simplest space filling molecular models for the fluid lamellar (A) and the inverse hexagonal phase (B). The models are derived from structural data of POPE at $T = 74\text{ }^{\circ}\text{C}$, at which the L_{α} -phase coexists with the H_{II} -phase [28]. (A) The steric length of a lipid molecule of 2.27 nm can be divided into headgroup extension, d_H (0.8 nm), and hydrocarbon chain length, ζ_0 (1.47 nm). The area per lipid was determined to be 0.65 nm^2 . (B) Simplest anisotropic molecular model for PE lipids in the inverted hexagonal phase. The different molecular areas are defined graphically, which are the lipid–water, the headgroup, the pivotal and terminal interface, respectively. Explicit values for the areas are given. Under the assumption that area per lipid at the headgroup position A_H is squared, it follows that about 19 lipid molecules are necessary for a full revolution in fully hydrated lipid cylinder (compare Fig. 7). Panel B is adapted from Ref. [34].

2.4. Models of Free Energy of the Inverted Hexagonal Phase

In general, solving the stability conditions for different lipid phases as well as conditions for the transition between lipid phases is a problem of defining the free energy of the system and its minimization. In the following a brief overview of theoretical models of L_{α} to H_{II} phase transition and the corresponding expression for the free energy of the system are described.

Kozlov *et al.* [24] studied the energy of the hexagonal phase in the H_{II} – L_{α} – H_{II} reentrant phase transition of dioleoylphosphatidylethanolamine (DOPE) upon changes in hydration and temperature. Combining osmotic stress and X-ray diffraction experiments, the spontaneous curvature (R_0^{-1}) and the monolayer bending constant (k_c) of the H_{II} phase were determined. Further, they considered a theoretical model describing the stability of hexagonal and lamellar lipid phases by minimization of the free energy consisting of elastic, hydration, interstitial, and van der Waals energies.

In the model of Kozlov and colleagues, the free energy of the hexagonal phase was approximated by the elastic energy of local bending deformation [37]:

$$F^H = N_1^H \frac{1}{2} k_c a_0 \left(\frac{1}{R} - \frac{1}{R_0} \right)^2 \quad (12)$$

where N_1^H is the number of lipid molecules, k_c is the bending elasticity of the lipid monolayer, a_0 is the area per lipid molecule, $1/R$ is the curvature of the pivotal plane of the lipid monolayer, and $1/R_0$ is the spontaneous curvature in fully hydrated (unstressed) state. For convenience, it was assumed that the free energy of fully hydrated hexagonal phase is 0 ($1/R = 1/R_0$) [24].

The free energy of the lamellar phase was assumed as follows:

$$F^L = N_1^L \frac{1}{2} P_0 \lambda a_0 M \exp\left(-\frac{d_w}{\lambda}\right) - N_1^L a_0 \frac{A_H}{24\pi d_w^2} + N_1^L a_0 \frac{1}{2} k_c \frac{1}{R_0^2} - N_1^L g_i \quad (13)$$

where N_1^L is the number of lipid molecules in the lamellar phase and d_w is the thickness of the water layer separating the bilayers. The first term is the energy of hydration repulsion between the bilayers (P_0 and λ are preexponential factor and characteristic length of the repulsion, respectively). The second term is the leading term in the energy of van der Waals interaction between the bilayers (A_H is the Hamaker constant [11]). The last two terms describe the difference between the free energies in the fully hydrated hexagonal and lamellar phases and give a constant contribution independent of the distance between the bilayers. The third term is the energy of “unbending” the lipid monolayer to flatness according to Eq. (12) and the last term represents the energy associated with voids in the hexagonal lattice. For simplicity $g_i > 0$ was referred as a curvature-independent part of the interstitial energy (curvature-dependent part is accounted for within the elastic energy of inverted hexagonal phase F^H (Eq. (12))) [24].

Kozlov *et al.* assumed that all parameters in Eqs. (12) and (13) except the intrinsic curvature R_0^{-1} are independent on temperature. By assuming a negligible dependence of g_i on temperature and equating the free energies in the hexagonal and lamellar phases in excess water in the temperature for reentrant transition ($T_H = 10^\circ\text{C}$) gives [24]

$$g_i = \frac{1}{2} k_c a_0 \frac{1}{[R_0(T_H)]^2} + \frac{1}{2} P_0 a_0 \lambda \exp\left(-\frac{d_{w\max}}{\lambda}\right) - \frac{a_0 A_H}{24\pi (d_{w\max})^2} \quad (14)$$

where N_1^L and N_1^H are taken to be equal and the free energy of the inverted hexagonal lipid phase is assumed to be $F^H = 0$ (i.e., $1/R = 1/R_0$), $d_{w\max}$

represents the equilibrium spacing in the lamellar phase in the absence of osmotic stress and T_H is the temperature of the hexagonal–lamellar reentrant transition in excess water. g_i was computed by introducing the measured parameters into Eq. (14) and is a positive constant in this case.

In summary, Kozlov *et al.* have described a model of L_α – H_{II} – L_α reentrant transition. On the basis of experiments, they have derived structural parameters and all of the force constants defining the energetic terms of the H_{II} and L_α lipid phases. They found an expression of interstitial energy of the inverted hexagonal phase as a constant difference between H_{II} and L_α phases at the transition point.

Another study on the hexagonal phase was performed by Rand *et al.* [38]. In this work, two types of energy contributions to the free energy of the lipid monolayer were taken into account:

$$G_{H_{II}} = \frac{1}{2} k_c a_0 \left(\frac{1}{R} - \frac{1}{R_0} \right)^2 + \Pi V_w \quad (15)$$

The first term in Eq. (15) introduces local bending energy and the second term is the osmotic energy, where k_c is the bending modulus, a_0 is the area per lipid molecule, R and R_0 are the actual local radii of the curvature and the intrinsic radius of curvature at the pivotal plane, respectively, Π is the difference in osmotic pressure between the outer bulk and inner confined solution, and V_w is the volume of water per lipid inside the cylinder [38]. Without consideration of the energy of interstices they made two approximations. The first approximation is that the water cylinders are perfectly circular in cross section (Fig. 9A). Second, the interstitial energy is proposed to be independent on the size of the hexagonal unit cell [38].

There exist two different approaches to express the interstitial (void) energy of the inverted hexagonal phase. In the first approach, rods of inverted hexagonal phase are assumed to be circular in cross section and the interstitial energy is assumed to be proportional to some imaginary surface of the voids between hexagonally packed cylinders [39] (Fig. 9A). In a second approach the interstitial energy was accounted in the terms of tilt and splay deformation of the phospholipid chains which have to fill the hexagonal unit cell while the cross section of neutral plane of lipid rods is assumed to be hexagonal [40] (Fig. 9B). Both approaches result in a proportionality constant by equating the free energies of the lamellar and inverted hexagonal phases at the transition temperature.

Malinin and Lentz [31] later improved the model of Rand *et al.* [38] (Eq. (15)), since the improved model included an energy cost due to voids (interstitial energy), see Fig. 9. To calculate the interstitial energy they assumed that the cross section of pivotal plane is intermediate between

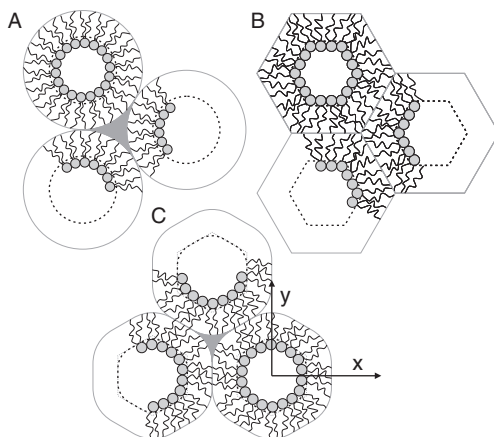


Figure 9 Schemes of different approaches to the expression of the free energy models of inverted hexagonal phase: (A) Circular cross section—Siegel [39] and Rand *et al.* [38], (B) hexagonal cross section—Hamm and Kozlov [40], (C) intermediate between circular and hexagonal cross section—Malinin and Lentz [31].

circular and hexagonal geometry (Fig. 9C), thus they parameterized the shape of the cross section:

$$y = \sqrt{d_p^2 - x^2} + \delta_0 \left(1 - \frac{4x^2}{d_p^2}\right)^2 \quad (16)$$

where x , y are coordinates of the pivotal plane, d_p is the distance from the axis of a rod to the pivotal plane in interaxial direction, and δ_0 is the maximal deviation from circular cylindrical geometry. Using Eq. (16) they computed the volumes of the water, voids, and the total unit cell volume. With assuming that the interstitial energy of inverted hexagonal phase is proportional to the volume of voids, the total free energy per lipid molecule is then derived as

$$g = \frac{A_0(K_b/2) \int_{-d_p/2}^{d_p/2} [(1/R_p) - (1/R_{p_0})]^2 \sqrt{1 + y'^2} dx}{\int_{-d_p/2}^{d_p/2} \sqrt{1 + y'^2} dx} \quad (17)$$

$$+ K_v V_v + \Pi V_w$$

where K_v is a proportionality coefficient representing the free energy of a unit of void volume, V_v and V_w are the volumes of the void and of the water, respectively and $dx\sqrt{1 + \gamma'^2}$ is the differential of the arclength [31].

The theoretical model of Malinin and Lentz included deviations from circularity in the inverted hexagonal phase cross section. The interstitial energy K_v (Eq. (17)) turned out to be constant, was derived from the volume of the voids in the hexagonal lattice.

In contrast to these models of interstitial energy g_i (Eq. (14)) and K_v in Eq. (17) we have expressed a relation for the interstitial energy dependent on stretching of the phospholipid chains on account to fill the voids directly. We also developed a new formalism to involve possible anisotropy of phospholipid shapes in our model calculations. In the following sections the new bottom up approach concerning the description of monolayer bending and packing frustration in the formation of the inverted hexagonal phase is outlined.

3. FREE ENERGY OF LIPID MONOLAYERS

It was shown in Ref. [24] that the free energy of the phospholipid monolayer in hexagonal phase may be expressed in terms of bending, interstitial, hydration, and van der Waals energy contribution. However, the contribution of the hydration energy in the excess water conditions is insignificant and also van der Waals energy only slightly contributes to the total free energy. Thus, we consider for the total free energy of the hexagonal phase two energy contributions: the energy of local bending and the interstitial energy (voids filling energy). Starting from a single molecule energy and applying the methods of statistical physics, the free energy of a lipid monolayer (bilayer) was derived [15, 21, 41, 42]. The local bending energy of laterally homogeneous monolayer (bilayer) [37, 43, 44] was recovered; however, an additional contribution due to average orientational ordering of lipid molecules, that is, the contribution of the deviatoric bending [45, 46] was included [15, 21, 42]. The average orientational ordering of anisotropic phospholipids lowers the free energy of the system; the effect is more pronounced for larger anisotropy of lipid molecules and stronger membrane curvature anisotropy [21].

3.1. Bending Energy of Lipid Monolayers

For better understanding we briefly repeat the derivation of the bending energy per lipid, which in general may be anisotropic [21]. This energy of a single lipid molecule depends on mismatch between curvature tensors \underline{C}_m (Eq. (9)) and \underline{C} (Eq. (2)). In general the curvature tensors \underline{C}_m and \underline{C} have

different orientations, that is, they are rotated by an angle ω . To express their mismatch we introduce the mismatch tensor \underline{M} :

$$\underline{M} = \underline{R}\underline{C}_m\underline{R}^{-1} - \underline{C} \quad (18)$$

where \underline{R} is transformation matrix for rotation:

$$\underline{R} = \begin{bmatrix} \cos \omega & -\sin \omega \\ \sin \omega & \cos \omega \end{bmatrix} \quad (19)$$

The single molecule energy at a given point of the membrane should be a scalar quantity, hence it may be expressed by two invariants of the tensor \underline{M} , trace, and determinant:

$$w_b = \frac{K_1}{2} \left(\text{Tr}(\underline{M}) \right)^2 + K_2 \text{Det}(\underline{M}) \quad (20)$$

where K_1 and K_2 are constants [21].

Eq. (20) can be rewritten as

$$\begin{aligned} w_b = & (2K_1 + K_2)(H - H_m)^2 \\ & - K_2 \left(D^2 - 2DD_m \cos(2\omega) + D_m^2 \right) \end{aligned} \quad (21)$$

where H is the mean curvature of a membrane (Eq. (3)), H_m is the mean intrinsic (spontaneous) curvature of the molecule (Eq. (10)), and D and D_m are the curvature deviators of the membrane and the molecule (Eqs. (5) and (11)), respectively [21]. In the following we introduce the definitions:

$$2K_1 + K_2 = \frac{\xi}{2} \quad \text{and} \quad K_2 = -\frac{\xi + \xi^*}{4} \quad (22)$$

Constants ξ and ξ^* describe the strength of intermolecular interactions. Using the definitions of ξ and ξ^* , Eq. (21) can be rewritten in the form

$$\begin{aligned} E(\omega) = & \frac{\xi}{2} (H - H_m)^2 \\ & + \frac{\xi + \xi^*}{4} \left(D^2 - 2DD_m \cos(2\omega) + D_m^2 \right) \end{aligned} \quad (23)$$

For sake of simplicity we assume that $\xi = \xi^*$. This equality yields $K_1 = -K_2$. It is obvious that the energy expressed by Eq. (23) reaches its minimum when $\cos(2\omega) = 1$ and its maximum when $\cos(2\omega) = -1$. In the first case the systems of tensors \underline{C}_m and \underline{C} are aligned ($\omega = 0$) or rotated by the angle $\omega = \pi$:

$$E_{\min} = \frac{\xi}{2}(H - H_m)^2 + \frac{\xi}{2}(D^2 + D_m^2) - \xi DD_m \quad (24)$$

while in the second case the systems are rotated by the angle $\omega = \pi/2$ or $\omega = 3\pi/2$:

$$E_{\max} = \frac{\xi}{2}(H - H_m)^2 + \frac{\xi}{2}(D^2 + D_m^2) + \xi DD_m \quad (25)$$

To derive the deviatoric bending energy of the whole monolayer, the membrane monolayer is divided into small patches that contain a sufficient large number of lipid molecules in order to apply the methods of statistical mechanics [21]. The principal curvatures C_1 and C_2 are taken to be constant over the patch and phospholipid molecules are considered to be equal and independent. Considering a simple two state model there are M equivalent molecules within the patch. Each molecule can exist in state of lower energy E_{\min} or higher energy E_{\max} . It means that N molecules are assumed to be in the state with E_{\max} and consequently $(M - N)$ molecules in the state with E_{\min} as shown in the next equation:

$$\frac{E_D}{kT} = N \frac{E_{\max}}{kT} + (M - N) \frac{E_{\min}}{kT} \quad (26)$$

where E_D is the deviatoric bending energy of the membrane patch. The energy of the patch is divided by k (Boltzmann constant) and T (thermodynamic temperature). Introducing Eqs. (24) and (25) into Eq. (26) gives

$$\frac{E_D}{kT} = M \frac{E_q}{kT} - \left(\frac{M}{2} - N \right) d_{\text{eff}} \quad (27)$$

where

$$\frac{E_q}{kT} = \frac{\xi}{2kT}(H - H_m)^2 + \frac{\xi}{2kT}(D^2 + D_m^2) \quad (28)$$

and

$$d_{\text{eff}} = \frac{(2\xi)D_m D}{kT} \quad (29)$$

d_{eff} is called the effective curvature deviator [21].

Another contribution to the bending energy is the direct interaction between molecules. At most the molecules interact with their nearest neighbors. It is assumed that if the actual shape of the membrane is in tune with the local curvature field, tails of the molecules move in average closer together and this leads to lowering energy. On the other side, if the molecules are oriented less favorable the average chain packing is less dense. This causes increasing of the energy. It is considered that this effect is proportional to d_{eff} (local effective curvature deviator). Direct interaction energy of N molecules that exhibit less favorable average packing is taken into account by the expression

$$\frac{E_N}{kT} = \frac{\tilde{k}}{kT} N d_{\text{eff}} \quad (30)$$

while the direct interaction energy of molecules that exhibit more favorable average packing (negative contribution) is described by

$$\frac{E_{M-N}}{kT} = -\frac{\tilde{k}}{kT} (M - N) d_{\text{eff}} \quad (31)$$

where \tilde{k} is the interaction constant [21].

The total energy caused by direct interaction is given by summation of Eqs. (30) and (31) divided by 2 as to avoid counting each molecule twice:

$$\frac{E_i}{kT} = -\frac{\tilde{k}}{kT} \left(\frac{M}{2} - N \right) d_{\text{eff}} \quad (32)$$

The total bending energy of the patch is thus

$$\frac{E^P}{kT} = \frac{E_D}{kT} + \frac{E_i}{kT} \quad (33)$$

where E_D/kT is the contribution of the average mutual orientation of the local curvature tensor and intrinsic curvature tensor (deviatoric bending) and E_i/kT is the contribution of the direct interaction between the neighbor molecules.

We consider all the patches to have a constant area A^P , a constant number of molecules M and a constant temperature T of the system.

The phospholipid molecules within the system are treated as indistinguishable. We assumed that the system is in thermodynamical equilibrium and only two states are possible just like in the description of a two-orientation model of noninteracting magnetic dipoles in the external magnetic field [47]. In our model the external magnetic field is represented by curvature deviator D [21]. By analogy, N molecules are in state with maximal energy and $(M - N)$ molecules are in state with minimal energy. The number of possibilities is $M!/N!(M - N)!$ while the corresponding energy is E^P . N can be any number from 0 to M . The canonical partition function $Q^P(M, T, D)$ of M molecule in the patch of the membrane is therefore

$$Q^P = \sum_{N=0}^M \frac{M!}{N!(M - N)!} \exp\left(-\frac{E^P}{kT}\right) \quad (34)$$

where k is the Boltzmann constant. Using Eqs. (27)–(34) gives

$$Q^P = q^M \sum_{N=0}^M \frac{M!}{N!(M - N)!} \exp\left(d_{\text{eff}} \left(1 + \frac{\tilde{k}}{kT}\right) \left(\frac{M}{2} - N\right)\right) \quad (35)$$

where by considering Eq. (28)

$$q = \exp\left(-\frac{E_q}{kT}\right) \quad (36)$$

Using the binominal (Newton) formula in summation of the finite series in Eq. (35) yields

$$Q^P = \left[2q \cosh\left(\frac{d_{\text{eff}} \left(1 + (\tilde{k}/kT)\right)}{2}\right) \right]^M \quad (37)$$

The Helmholtz free energy of the patch is $F^P = -kT \ln Q^P$. Combining Eqs. (35)–(37) yields the free energy of the patch:

$$F^P = M \frac{\xi}{2} [(H - H_m)^2 + D^2 + D_m^2] - kTM \ln \left[2 \cosh\left(\frac{\left(1 + (\tilde{k}/kT)\right) \xi D_m D}{kT}\right) \right] \quad (38)$$

The bending energy of the monolayer is given by the summation of the contributions of the all patches of the monolayer, i.e. integration is performed over the whole area A :

$$F_b = \int_A \frac{n_0 \xi}{2} [(H - H_m)^2 + D^2 + D_m^2] dA - n_0 kT \int_A \ln \left[2 \cosh \left(\frac{\xi \left(1 + (\tilde{k}/kT) \right) D_m D}{kT} \right) \right] dA \quad (39)$$

where n_0 is the area density of the lipid molecules, ξ is the constant describing the strength of the interaction between a single lipid molecule and the surrounding membrane continuum, k is the Boltzmann constant, T is temperature, \tilde{k} is the constant describing the direct interaction between lipid molecules [21], and dA is the area element of the lipid monolayer.

If we consider surfaces with small curvature deviators D or molecules with small D_m , we can substitute the term $\ln(\cosh(x))$ in Eq. (39) by the first term in Taylor expansion: $\ln(\cosh(x)) \cong \ln(1 + x^2/2) \cong x^2/2$. Thus, our general expression for monolayer bending energy transforms into Helfrich expression for local bending energy of lipid monolayer [37]:

$$w_b = \frac{k_c}{2} (2H - C_0)^2 + k_G K \quad (40)$$

where w_b is the area density of the monolayer bending energy, while the constants k_c , k_G , and C_0 are defined as

$$k_c/n_0 = \frac{\xi}{2} - \frac{(1 + \tilde{k}/kT)^2 \xi^2 D_m^2}{4kT} \quad (41)$$

$$k_G/n_0 = -\frac{\xi}{2} + \frac{(1 + \tilde{k}/kT)^2 \xi^2 D_m^2}{2kT} \quad (42)$$

and

$$C_0 = H_m \left[1 + \frac{[1 + (\tilde{k}/kT)]^2 \xi D_m^2}{2kT} \right] \quad (43)$$

The constant C_0 represents spontaneous (intrinsic) curvature of the lipid monolayer.

In the simplest case, where only isotropic phospholipid molecules within the lipid monolayer are taken into account ($D_m = 0$), the constants are defined as

$$k_c/n_0 = \frac{\xi}{2} \quad (44)$$

$$k_G/n_0 = -\frac{\xi}{2} \quad (45)$$

while the expression for the spontaneous (intrinsic) curvature is equal to the mean curvature of the lipid monolayer:

$$C_0 = H_m \quad (46)$$

3.2. Interstitial Energy of the Inverted Hexagonal Phase

In this section we are interested in the derivation of a dependence for an energy contribution from “voids”—interstitial energy, which was already discussed in Section 2.2 [1, 24, 31]. The need of additional interstitial energy contribution in the H_{II} phase appears due to the special packing geometry of the inverted hexagonal phase (compare with Section 2).

In the lamellar phase L_α , the monolayers have a constant thickness and there are no voids in the mid-plane of the bilayer. On the other hand, in the inverted hexagonal phase, the distance between two adjacent monolayers varies over the monolayer surface. Some of the lipid tails have more space, while others are squeezed with respect to an average length ζ_0 (Fig. 6). To avoid water pockets, the hydrocarbon tails of lipid molecules have to stretch accordingly. The void-filling energy contribution due to lipid stretching can be expressed on the basis of Hooke's law [48]:

$$f_d = \tau(\zeta - \zeta_0)^2 \quad (47)$$

where ζ is the actual length of the fatty acid chain and τ is the proportionality constant reflecting the stiffness of the chains (stretching modulus). We suppose that the area density of the contact energy is given as

$$\lambda_c = \tau(\zeta - \zeta_0)^2 n_0 \quad (48)$$

where n_0 is the area density of phospholipid molecules ($n_0 = 1/a_0$). The total contact energy is given as

$$F_i = \int_A \lambda_c dA \quad (49)$$

where we integrate over the whole area of lipid monolayer A . The Eq. (49) can be written in the form

$$F_i = Y\tau n_0 \int_l (\zeta - \zeta_0)^2 dl \quad (50)$$

where dl is the element of the length of the curve corresponding to phospholipid monolayer in the projection of hexagonal phase shown in Fig. 6 and Y is the length of the inverted hexagonal tube.

To estimate the actual length of hydrocarbon chain ζ , cylindrical coordinates are introduced. The length of hydrocarbon chains may be estimated from hexagonal geometry of the lattice. From the rectangular triangle depicted in Fig. 10 it follows:

$$\zeta = \frac{a}{2 \cos \varphi} - r \quad (51)$$

Because of hexagonal symmetry, Eq. (51) is valid for the contact region of two adjacent lipid cylinders, that is, for 1/12 of the area of one lipid cylinder. The values of the angle φ are therefore defined in the range of

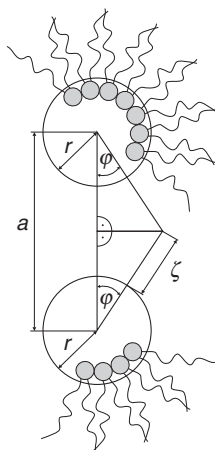


Figure 10 Scheme of two neighboring inverted lipid tubes in hexagonal lattice. The lipid tails have to stretch in order to fill voids in the hydrocarbon region. The symbol a denotes the H_{II} phase lattice constant and r denotes the radius of the pivotal plane of the H_{II} phase. The actual length of hydrocarbon tails (ζ) depends on the angle φ .

$$\varphi \in \left[0, \frac{\pi}{6}\right] \quad (52)$$

If $\varphi = 0$, the length of hydrocarbon chains ζ is equal to $(a/2) - r$. At the upper limit of the range of φ , the length of the hydrocarbon chain is equal to $(a/\sqrt{3}) - r$.

Considering the cylindrical transformation ($r d\varphi = dl$), the symmetry of the problem (12 identical segments) and the expression for the length of hydrocarbon chains (Eq. (51)), Eq. (50) can be written in the form

$$F_i = Y\tau n_0 12r \int_0^{\pi/6} \left(\frac{a}{2 \cos \varphi} - r - \zeta_0 \right)^2 d\varphi \quad (53)$$

After solving the integral in Eq. (53), the contact energy of one lipid cylinder (Eq. (53)) can be written as

$$F_i = 12Y\tau n_0 r \left(\frac{a^2 \sqrt{3}}{12} - a(r + \zeta_0) \ln \sqrt{3} + \frac{\pi}{6} (r + \zeta_0)^2 \right) \quad (54)$$

3.3. Total Free Energy per Lipid Molecule

The total free energy per lipid molecule in inverted hexagonal phase can be computed as

$$f = \frac{E}{M} \quad (55)$$

where M is the total number of lipid molecules in the system with energy E . The total number of molecules can be calculated from the total area of membrane A and the area corresponding to one lipid molecule (a_0), that is, the area density of the lipid molecule (n_0):

$$M = \frac{A}{a_0} = n_0 A \quad (56)$$

The total area of one lipid cylinder in the inverted hexagonal phase is

$$A = 2\pi r Y \quad (57)$$

From summation of Eqs. (39) and (49) it follows that the free energy per lipid molecule in the H_{II} phase can be expressed as

$$\begin{aligned}
 F = \frac{F_b + F_i}{2\pi n_0 Yr} = \frac{\xi}{2} [(H - H_m)^2 + D^2 + D_m^2] \\
 - kT \ln \left[2 \cosh \left(\frac{\left(1 + (\tilde{k}/kT)\right) \xi D_m D}{kT} \right) \right] \\
 + \frac{6}{\pi} \tau \left(\frac{a^2 \sqrt{3}}{12} - a(r + \zeta_0) \ln \sqrt{3} + \frac{\pi}{6} (r + \zeta_0)^2 \right)
 \end{aligned} \quad (58)$$

Equations (1) and (3) yield for cylindrical geometry of the H_{II} phase $H = -1/2r$ and $D = |H|$. The first two terms in Eq. (58) represent the bending energy contribution and the third term is interstitial energy contribution to the free energy.

4. ESTIMATION OF MODEL CONSTANTS

In order to determine the free energy of different configurations of the lipid monolayers, the values of the model constants were estimated. The value of interaction constant ξ was estimated from monolayer bending constant $\xi = 2k_c a_0$, where for POPE $k_c = 11kT$ is the bending constant [49] and $a_0 = 0.65 \times 10^{-18} \text{ m}^2$ is the area per phospholipid molecule [28]. The reference (nonstretched) length of the phospholipid tails ζ_0 (Fig. 6) was taken to be 1.30 nm [28]. In calculation of the interstitial energy the lipid stretching modulus τ was taken to be in the range from $0.95kT \text{ nm}^{-2}$ to $95kT \text{ nm}^{-2}$ (see Ref. [48]). For the sake of simplicity it was taken that the molecules favor cylindrical geometry, that is $|H_m| = D_m$. The effect of the temperature was simulated by increasing the intrinsic curvatures $|H_m|$ and D_m with increasing temperature which is consistent with increased spreading of the phospholipid tails while the headgroup extensions in POPE remain relatively unchanged. The range of the intrinsic curvatures was taken to be from 0 to 0.4 nm^{-1} , corresponding to curvature radii down to 1 nm. To study the effect of the deviatoric bending, also the hypothetical case where the molecules are isotropic ($D_m = 0$) was considered.

5. DETERMINATION OF EQUILIBRIUM CONFIGURATION OF PLANAR AND INVERTED CYLINDRICAL SYSTEMS

5.1. Numerical Solution

To show the importance of the interstitial energy, we compare three different geometries of lipid monolayers: planar, cylindrical, and spherical. The systems were described as surfaces with constant principal curvatures. In the planar system, $H = D = 0$, in the inverted spherical system $H = -1/r_s$ and $D = 0$, while in the inverted cylindrical system $H = -D = -1/2r$, where r is the radius of the cylinder and r_s is the radius of the sphere. The minimal value of the free energy of a unit patch of the lipid monolayer with respect to the mean curvature H was calculated by using Eq. (58) while the model constants are given in Section 4.

5.2. Results of Equilibrium Configurations of Planar and Inverted Cylindrical Systems

To explain the effect of individual contributions to the free energy, we first determine the equilibrium configuration obtained by minimization of the bending energy alone (first two terms in Eq. (58)). There are three different geometries compared in Fig. 11: planar (corresponding to lamellar L_α phase), spherical (corresponding to inverted micellar M_{II} phase), and cylindrical (corresponding to inverted hexagonal H_{II} phase), see also Fig. 1. Figure 11 shows the equilibrium bending energy per lipid molecule dependent on the mean intrinsic curvature H_m for anisotropic molecules, for which $|H_m| = D_m$ (panel A) and isotropic molecules, for which $D_m = 0$ (panel B). For small $|H_m| = D_m$, the bending energy increases with increasing $|H_m|$ in all three geometries (panel A). In the M_{II} and L_α phases, which are isotropic with respect to the curvature ($D = 0$), there is no orientational ordering of the molecules and the bending energy monotonously increases also for larger $|H_m| = D_m$. In the H_{II} phase, however, the nonzero values of both the intrinsic curvature deviator D_m and the curvature deviator D give rise to a negative energy contribution of the deviatoric bending. Therefore, the equilibrium free energy reaches a maximum upon an increase of D_m (which for this particular choice of molecules it is equal to $|H_m|$), but then decreases at a certain threshold, and such the H_{II} phase becomes energetically the most favorable. Summing up, for small $|H_m| = D_m$, the M_{II} phase has the lowest bending energy, while at larger $|H_m| = D_m$, the H_{II} phase becomes the most favorable due to the average orientational ordering of phospholipid molecules. The effect is stronger for higher values of \bar{k} describing the direct interaction between phospholipid tails (Fig. 11A).

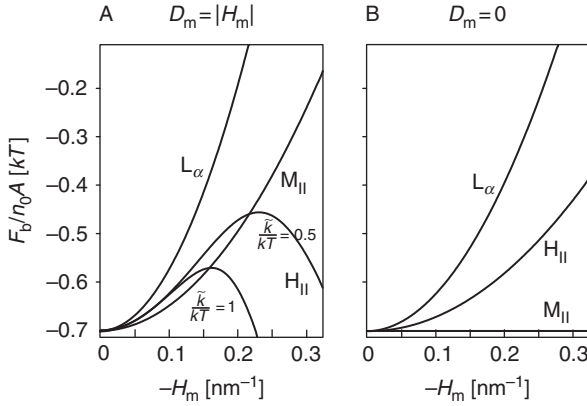


Figure 11 The equilibrium bending energy per lipid molecule F_b/n_0A in dependence on the intrinsic mean curvature H_m for the L_α , M_{II} , and H_{II} phases: (A) a system composed of anisotropic molecules ($D_m = |H_m|$) and (B) a system composed of isotropic molecules ($D_m = 0$). For the bending contribution, see Eq. (58). Adapted from Ref. [29].

Figure 11B shows that for isotropic molecules (having $D_m = 0$, i.e., $C_{1m} = C_{2m}$, see also Fig. 2), the M_{II} phase is always favored, that is, the calculated energy per lipid F_b/n_0A in the M_{II} phase is equal to the reference value and is the smallest comparing to the energy of the L_α and the H_{II} phase. We note that for isotropic molecules there can be no energy lowering due to the average orientational ordering of the molecules since all orientations of the lipid molecules are energetically equivalent.

The deviatoric bending of anisotropic molecules may thus alone explain the stability of the H_{II} phase at higher temperatures. At lower temperatures, the M_{II} phase is energetically favored except for $|H_m| = D_m = 0$, where the L_α phase is the stable phase. At small $|H_m| = D_m$, however, the equilibrium radii of the simulated M_{II} phase are so large that this case would correspond to flat membrane systems. For some intermediate $|H_m| = D_m$, the simulated M_{II} phase would consist of aggregated micelles of a given size, however such a configuration is actually not observed [50, 51].

To obtain a better agreement with experimental observations also in the intermediate range of $|H_m| = D_m$, we include the effect of void filling energy by using a simple model, where the void-filling energy is considered constant for a given geometry (see also Ref. [24]). Figure 12 shows the minimal free energy $F/n_0A = F_b/n_0A + F_i/n_0A$ in dependence on the intrinsic mean curvature H_m for the L_α , H_{II} , and M_{II} phases. Here F_i is the interstitial energy, n_0 is the area density of the lipid molecule, and A is the area of the whole monolayer (see Eqs. (39) and (54)). Since the energy contribution of voids is smaller in the system of close packed inverted

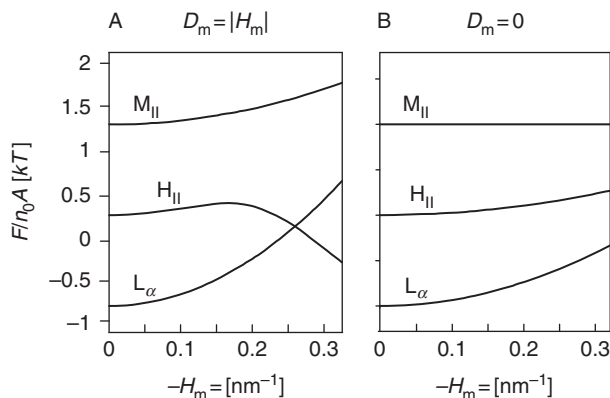


Figure 12 The equilibrium free energy per lipid molecule $F_b/n_0 A + \chi$ consisting of the contribution of bending and of a constant for the void filling energy per lipid molecule in dependence on the intrinsic mean curvature $|H_m|$ for the L_α ($\chi = 0$), H_{II} ($\chi = 1kT$) and M_{II} ($\chi = 2kT$) phases: (A) $D_m = |H_m|$ and (B) $D_m = 0$, $k/kT = 1$. Adapted from Ref. [29].

cylinders than in the system of close packed inverted spheres, the value of the void-filling energy per lipid molecule $F_i = \chi$ was taken to be lower for cylinders than for spheres. It was estimated from the results of Kozlov *et al.* [24] that χ should be of the order of kT [24], therefore we took for the H_{II} phase $\chi = 1kT$ and for the M_{II} phase $\chi = 2kT$.

In Fig. 12A and B the curves corresponding to the H_{II} and M_{II} phases in Fig. 11 are shifted up for different constants χ , respectively, and the overall picture is now more realistic. It can be seen in Fig. 12A and B that for small $D_m = |H_m|$ the L_α phase is energetically the most favorable, since it requires no void-filling energy. For anisotropic molecules (Fig. 12A) at a certain threshold $D_m = |H_m|$, the H_{II} phase becomes energetically the most favorable due to the average orientational ordering of the lipid molecules. In the isotropic case (Fig. 12B), all curves monotonously increase; however, the curve corresponding to the L_α phase increases faster and therefore it would eventually cross with the curve corresponding to the H_{II} phase. However, the value of H_m where the intersection would take place would be very high (out of range given in Fig. 12, where the maximal value 0.4 nm^{-1} already corresponds to a cylinder with a radius of only 1.25 nm).

In short, the effects shown in Fig. 12A indicate that in the simple model where the interstitial energy is taken to be constant within a phase [24, 29], an increase of $D_m = |H_m|$, which is caused by the increase of temperature can induce the transformation from L_α to H_{II} lipid phase. Taking into account the interstitial energy for small $|H_m|$ (lower temperature) renders, the L_α phase is energetically the most favorable, while at a certain threshold

$D_m = |H_m|$ (higher temperature), the H_{II} phase becomes energetically the most favorable.

Having eliminated the M_{II} phase due to high packing frustration (Fig. 12), in the following, we compare only the L_α and the H_{II} phases by using an improved model for the void filling energy, where stretching of the lipid tails in the actual hexagonal geometry is taken into account (Fig. 6 and Eq. (52)). Figure 13 shows the free energy per lipid molecule F/n_0A in dependence on the intrinsic mean curvature H_m for the L_α and the H_{II} phase.

We can compare the total free energy per molecule for anisotropic and isotropic phospholipid molecules in dependence on the mean intrinsic curvature H_m . It can be seen in Fig. 13 that there are three curves corresponding to the inverted hexagonal phase with different stiffness constants τ and one curve corresponding to the lamellar phase. For stiff hydrocarbon chains (high values of τ), the lamellar phase has lower energy than the inverted hexagonal phase, while for decreasing τ , the inverted hexagonal phase is energetically more favorable than the lamellar phase for high enough $|H_m|$. Isotropic lipid molecules in the inverted hexagonal phase also exhibit the lowest energy for less stiff hydrocarbon chains.

By comparing Fig. 13A and B, it is important to point out that the anisotropy of phospholipid molecules evokes a steeper increase of the absolute value of the energy difference between the lamellar and the inverted hexagonal phases with temperature and therefore promotes and stabilizes the H_{II} phase profoundly.

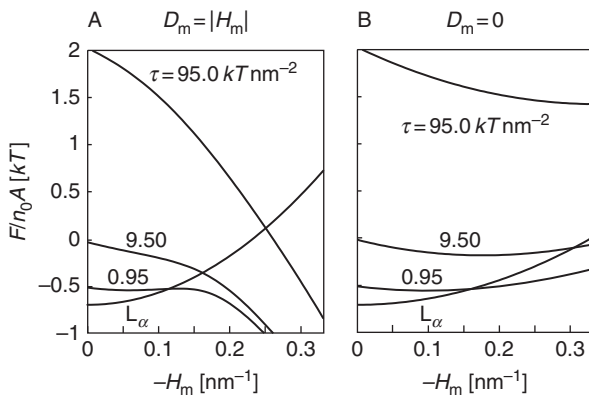


Figure 13 Free energy per lipid molecule F_b/n_0A consisting of the bending and the interstitial contributions in dependence on the intrinsic mean curvature of lipid molecules $|H_m|$ in the L_α and H_{II} phase for various stiffnesses of hydrocarbon chains τ for (A) $|H_m| = D_m$ and (B) $D_m = 0$. See Eq. (58). $\bar{k}/kT = 1$. Adapted from Ref. [29].

For a more detailed study of the H_{II} phase we have constructed graphs its structural parameters. Figure 14 shows the dependence of the cylinder radius r and of the distance between the centers of the lipid cylinders a , respectively, (Fig. 6), on the intrinsic curvature $|H_m|$ for three values of τ of anisotropic lipid molecules. The H_{II} phase is composed of lipid cylinders with small radius r and small separation a for lipids of large mean intrinsic curvatures. Decreasing the absolute value of the mean intrinsic curvature $|H_m|$ increases both the radius of the H_{II} cylinders and the lattice length. However, cylinders of large radii increase the void space and the corresponding stretching of hydrocarbon chains. Therefore, the maximum radii of the cylinders are limited by the energy of interface region between the cylinders. If the hydrocarbon chains are stiff (large value of τ), the creation of voids is energetically unfavorable. In this case, the small radii of cylinders are preferred as they provide small void spaces (Fig. 14A). On the other hand, if the stretching of hydrocarbon chains does not require much energy (small τ), larger radii of hydrocarbon chains are permitted.

It is instructive to compare the given plots with experimental data [28, 34] (Fig. 14, dashed lines). First, it teaches us that realistic value of the stretching moduli τ most probably lie between 0 and $20kT \text{ nm}^{-2}$ (for large enough τ , e.g., $\tau = 95kT \text{ nm}^{-2}$ no realistic dimensions of the H_{II} lattice can be predicted). Second, the range of realistic intrinsic mean curvatures $-H_m$ lies probably in the range of $0.1\text{--}0.2 \text{ nm}^{-1}$. Note that this comes close to the value of the mean curvature $-H$ of the POPE/water system (Table 1) and is also in agreement with values of intrinsic curvatures of lipids given by other authors [52]. The effect of contact energy in the

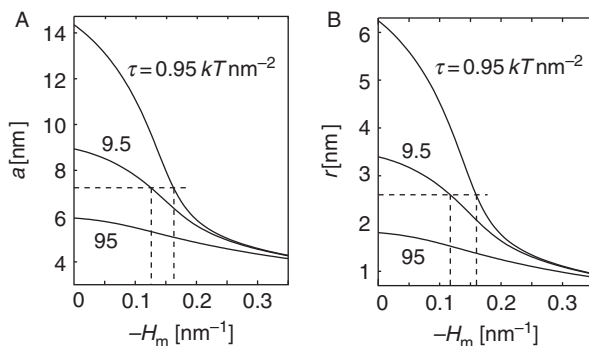


Figure 14 Structural parameters of the H_{II} phase for the case where $D_m = |H_m|$. (A) The optimal unit cell parameter a and (B) the optimal pivotal plane radius r (core center to polar/apolar interface) are plotted versus the absolute value of the mean curvature H_m for different lipid chain rigidities τ . The two horizontal dashed lines mark the realistic values for a and r , respectively (Table 1). For definitions of a and r , see Fig. 6. $\bar{k}/kT = 1$. Adapted from Ref. [29].

Table 1 Geometrical parameters of the L_α and the H_{II} phases at $T = 74^\circ\text{C}$

Parameter	$L_\alpha = 74^\circ\text{C}$	$H_{II} = 74^\circ\text{C}$
D, a (nm)	4.99	7.24
d_{pol}, r (nm)	2.5	2.67
ζ_0 ($\zeta_{\text{min}}, \zeta_{\text{max}}$) (nm)	1.47	1.13 (0.95, 1.51)
a_0 (nm^2)	0.65	0.65
H (nm^{-1})	0	0.187

The structural parameters are defined in Fig. 6. The experimental values are taken from Ref. [28].

stabilization of the hexagonal phase is obvious if the value of τ is large enough. Large diameter of the lipid cylinder r produces larger voids that are energetically unfavorable.

5.3. Influence of the Direct Interaction Constant \tilde{k}

Figure 15 shows the effect of the direct interaction constant \tilde{k} [21] on the calculated free energy per lipid molecule. The energy \tilde{k}/kT was estimated by the van der Waals interactions between the tails of orientationally ordered and orientationally disordered nearest neighbors of a given molecule [21].

It can be seen in Fig. 15 that for low values of \tilde{k}/kT the behavior of the anisotropic lipid molecules in our theoretical model are energetically close to the behavior of isotropic molecules.

6. LAMELLAR TO INVERTED HEXAGONAL PHASE TRANSITION

6.1. Determination of Pivotal Map of Nucleation Contour by Minimization of Monolayer Bending Energy

Following the nucleation model of the L_α - H_{II} transition given in [28, 34], the surface of the monolayer forming a closure is described by the radius vector $\mathbf{r} = (x, y, z(x))$ (Figs. 7 and 16), wherefrom the mean and the Gaussian curvatures are

$$2H = \frac{-\frac{\partial^2 z}{\partial x^2}}{\left(1 + \left(\frac{\partial z}{\partial x}\right)^2\right)^{3/2}} \quad (59)$$

and

$$C_1 C_2 = 0 \quad (60)$$

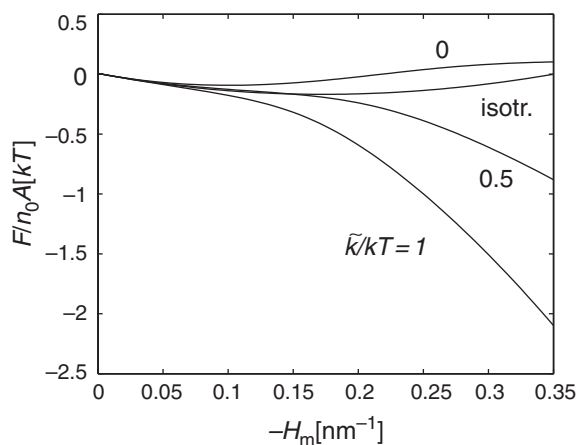


Figure 15 Influence of the direct interaction constant \tilde{k} on the calculated free energy per lipid molecule F/n_0A in the H_{II} phase. Comparison with free energy per isotropic phospholipid molecule is given.

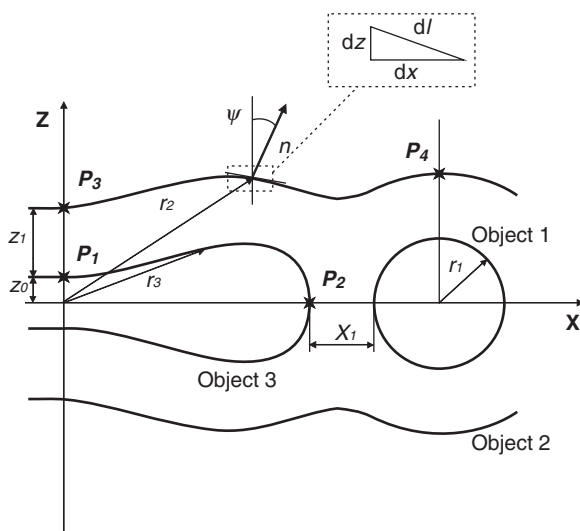


Figure 16 Parametrization of the pivotal surface. Two bulby closures (objects 3) are placed between adjacent bilayers (objects 2) and a cylinder (object 1). The geometry of the system is symmetrical with respect to the x -axis.

The surface is given in terms of the arclength l , so that $\sin \psi = dz/dl$ and $\cos \psi = dx/dl$. Considering the above definitions, the mean curvature is expressed as $2H = 2D = d\psi/dl$, while the area element is $dA = Y dl$. Due to

symmetry, only the part of the contour above the x -axis is considered in determination of the equilibrium shape of the closure.

The coordinates, the area, the area element, and the bending energy are written in dimensionless form. Normalizing the curvatures and distances by an arbitrary unit of length z_0 (in our case we set $z_0 = 1$ nm) gives dimensionless curvatures:

$$h = z_0 H, \quad d = z_0 D, \quad h_m = z_0 H_m, \quad d_m = z_0 D_m \quad (61)$$

and a dimensionless arclength:

$$\tilde{l} = \frac{l}{z_0} \quad (62)$$

The area element is normalized to Yz_0 . The bending energy is normalized to $n_0 \xi Y / 2z_0$:

$$f_b = \int (\zeta - \zeta_m)^2 d\tilde{l} + \int (d^2 + d_m^2) d\tilde{l} - \kappa \int \ln[2 \cosh[(1 + (\tilde{k}/kT)) \vartheta 2d_m d]] d\tilde{l} \quad (63)$$

where

$$\kappa = \frac{1}{\vartheta} = \frac{2kTz_0^2}{\xi} \quad (64)$$

To minimize the bending energy (63), a functional

$$L = \left(\frac{1}{2} \frac{d\psi}{d\tilde{l}} - \zeta_m \right)^2 + \frac{1}{4} \left(\frac{d\psi}{d\tilde{l}} \right)^2 - \kappa \ln \left(2 \cosh \left((1 + \tilde{k}/kT) \vartheta 2d_m d \right) \right) - \lambda \left(\cos \psi - \frac{dx}{d\tilde{l}} \right) - \nu \left(\sin \psi + \frac{dz}{d\tilde{l}} \right) \quad (65)$$

is minimized by solving a system of Euler–Lagrange equations:

$$\frac{\partial L}{\partial \psi} - \frac{d}{d\tilde{l}} \left(\frac{\partial L}{\partial \psi_{\tilde{l}}} \right) = 0 \quad (66)$$

$$\frac{\partial L}{\partial x} - \frac{d}{d\tilde{l}} \left(\frac{\partial L}{\partial x_{\tilde{l}}} \right) = 0 \quad (67)$$

$$\frac{\partial L}{\partial z} - \frac{d}{d\tilde{l}} \left(\frac{\partial L}{\partial z_{\tilde{l}}} \right) = 0 \quad (68)$$

where $\psi_{\tilde{l}} = d\psi/d\tilde{l}$, $x_{\tilde{l}} = dx/d\tilde{l}$, and $z_{\tilde{l}} = dz/d\tilde{l}$. By introducing the variable

$$Y = x \frac{d\psi}{d\tilde{l}} \quad (69)$$

a system of equations (66)–(68) yields

$$\frac{dY}{d\tilde{l}} = \frac{Y}{x} \cos \psi + \frac{(\lambda \sin \psi - v \cos \psi)x}{1 - \left[(\kappa \tilde{\vartheta}^2 d_m^2) / (\cosh^2(\tilde{\vartheta} d_m Y/x)) \right]} \quad (70)$$

$$\lambda = \text{const}, \quad v = \text{const}, \quad \tilde{\vartheta} = \vartheta \left(1 + \frac{\tilde{k}}{kT} \right) \quad (71)$$

where λ and v are local Lagrange multipliers. The system of equations (70)–(71) was solved numerically by using the Merson method to yield the equilibrium contour map of the pivotal plane of the bulby closure as shown in Fig. 16.

6.2. Determination of Equilibrium Configuration of Lamellar to Inverted Hexagonal Phase Transition by Monte Carlo Simulated Annealing Method

The configuration of monolayers adjacent to the central cylinder representing a nucleation line for the L_α – H_{II} phase transition is described by the radius of the central cylinder and a set of N angles, ψ_i , $i = 1, 2, \dots, N$, describing the bulby closure and the surrounding monolayers (Fig. 16), which were divided into N sufficiently small parts. The boundary conditions were introduced to reflect connections within the different parts of the system. Due to symmetry, this unit includes a quarter of the cylinder, half of the bulby closure and one neighboring monolayer.

The minimization of the free energy of the system was performed by the Monte Carlo simulated annealing sampling strategy [53]. The method was invented by Kirkpatrick *et al.* [53] as an adaptation of the Metropolis–Hastings algorithm, which constitutes the Monte Carlo method [54]. The method is inspired by physical process of annealing in metallurgy, when the heating and subsequent slow cooling of a material is used for the increase of the crystal size in the material and thus reduces defects.

By analogy of this effect, each step of the simulated annealing algorithm moves the current solution to a sufficiently near random solution. The probability of accepting of a new solution depends on the difference in the corresponding function values and a global parameter T (temperature), which is decreasing during the process under a cooling schedule. For high values of temperature the randomness of the choice is considerable, thus the solution can jump out from local minima. With decreasing of temperature the probability for acceptance of a solution corresponding to higher energy is decreased, hence the solution is smoothed in a low temperature mode.

Within this approach, it is assumed that any local minimum is accessible from any other minimum after a finite number of random sampling steps [54]. In contrast to the conventional Metropolis Monte Carlo method, all values of angles ψ together with the radius of the central cylinder r were updated in each step [53]. After each step, the total free energy of the system was evaluated by the Metropolis criterion [54] and compared with the free energy of the previously accepted state. To find the global minimum in the multivariational space, the simulation was started at sufficiently high temperature according to the Metropolis criterion, while according to the cooling schedule the temperature was decreased after each step until it reached the zero value.

The initial configuration of the system composed of the contour shape of the bulby closure was determined by solving the Euler–Lagrange equations, the radius of the central cylinder was determined by the maximal value of z coordinate of this bulby closure, and two adjacent flat monolayers sandwiching the bulby closure and the cylinder were taken as a first approximation in the procedure of the energy minimization by the Monte Carlo simulation annealing method. This choice of the initial configuration considerably increased the speed of the time-consuming Monte Carlo simulated annealing method.

6.3. Results: Equilibrium Configuration of Nucleation of the Lamellar to Inverted Hexagonal Phase Transition

Solving the equilibrium configuration of the system with an inverted cylinder surrounded by two monolayers and two bulby closures yielded results depicted in Figs. 17 and 18.

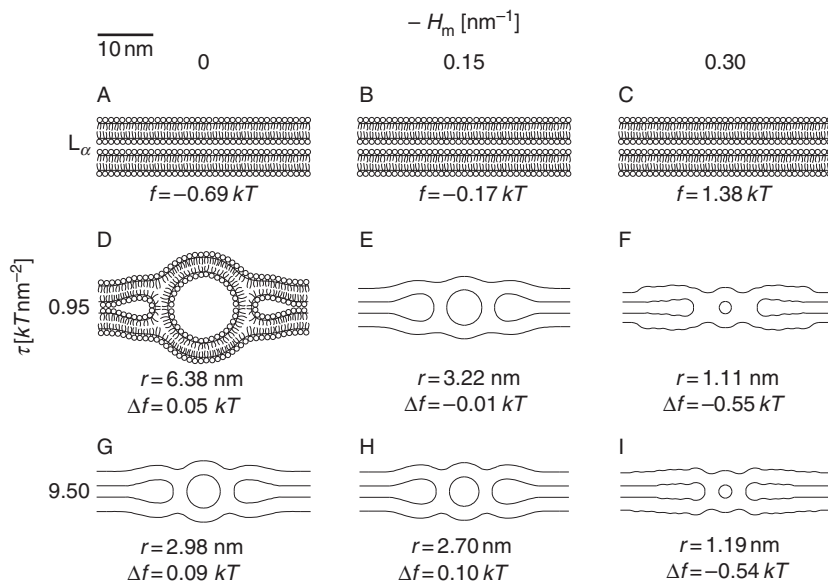


Figure 17 Configuration of the system of two monolayers, a first cylinder of H_{II} phase and two bulby closures representing a nucleation line in the L_{α} - H_{II} transition for different intrinsic curvature H_m and different stretching moduli of the phospholipid chains τ . We assume that phospholipid molecules are anisotropic corresponding to $D_m = |H_m|$. The free energy per lipid molecule and the radius of the central cylinder are given for each configuration. Adapted from Ref. [29].

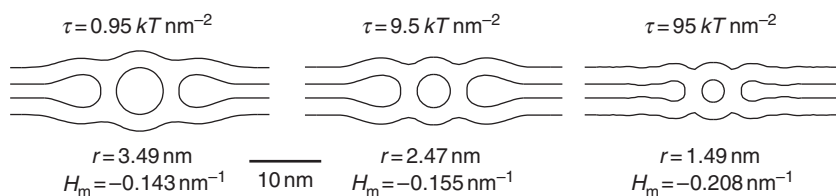


Figure 18 Nucleation configurations for different values of stretching modulus of phospholipid tails (τ) at transition point from L_{α} to H_{II} phase where $\Delta f = 0$. Anisotropic case ($D_m = |H_m|$). Adapted from Ref. [29].

In Fig. 17, snapshots of the equilibrium configurations for anisotropic phospholipids (setting $D_m = |H_m|$) and different values of model parameters are displayed. The top row presents the L_{α} phase with values of the free energy per lipid molecule of the pure L_{α} phase. The next two rows show the equilibrium configuration of the system with the first cylinder of the H_{II} phase embedded between two monolayers. The energy of these structures is

described by energy difference $\Delta f = f_{H_{II}} - f_{L_\alpha}$, where $f_{H_{II}}$ is the energy per lipid molecule in the hexagonal phase and f_{L_α} is the energy per lipid molecule in the lamellar phase at given values of model constants. From top to bottom, the stretching modulus of the phospholipids is increased: $\tau = (0.95 \text{ and } 9.5) kT \text{ nm}^{-2}$. From left to right the lipid intrinsic mean curvature $|H_m| = 0$ is increased: $|H_m| = (0, 0.15, 0.3) \text{ nm}^{-1}$.

It can be seen in Fig. 17 that the inverted hexagonal phase (H_{II}) configuration is energetically more favorable than the pure lamellar L_α phase at sufficiently high values of the mean intrinsic curvature $|H_m|$. In the model increase of the temperature is simulated by increasing of $|H_m|$. For higher values of the mean intrinsic curvature $|H_m|$, the energy difference Δf decreases, thereby the configuration with the cylinder is favored. This phenomenon is in accordance with experimental results showing that the formation of the H_{II} phase is promoted with increasing temperature [28].

It is evident from Fig. 17 that the radius of the cylinder r decreases with increasing stretching modulus of the phospholipid chains τ and increasing $|H_m|$ which is in agreement with the results presented in Fig. 14. Creation of a cylinder in the lamellar phase becomes less disturbing for adjacent lipid layers when the radius of the cylinder r is decreased enough.

For high enough values of τ there is a negligible effect of H_m on the equilibrium radius of the central cylinder r because the stretching modulus τ plays a considerable role in the energy balance and also because the contact energy is much higher than the bending energy. On the other hand small τ means a low contact energy that cannot compete with the bending energy. Consequently, the radius of the central cylinder r approaches $r_m = 1/H_m$.

The transition from the L_α to H_{II} phase in the nucleation model occurs at the energy difference $\Delta f = 0$, that is, when the energy of H_{II} phase is equal to energy of L_α phase for $|H_m| = D_m$, (Fig. 18). By comparison of three different configurations of H_{II} phase nucleation corresponding to different phospholipid chain stiffness, one can see that for low τ the L_α - H_{II} transition takes place for smaller $|H_m|$ and the predicted radius of initial cylinder does not have a realistic value ($r = 3.49 \text{ nm}$), that is, it is much larger than the experimental values [28, 34]. However, for larger values of τ the calculated r corresponds to experimental values much better. At $|H_m| = 0.155 \text{ nm}^{-1}$ the nucleation cylinder radius is 2.47 nm , which agrees well with data obtained from X-ray experiments [28, 49]. As the decrease of the free energy with increasing $|H_m|$ is more pronounced in the pure hexagonal phase (Fig. 13) than in the nucleation configuration (Fig. 18), the values of τ around $9.5 kT \text{ nm}^{-2}$ would lead to the stabilization of the H_{II} phase at higher temperatures. For large τ (e.g., $\tau = 95 kT \text{ nm}^{-2}$), the predicted nucleation transition is again less realistic due to the too small value of $r = 1.49 \text{ nm}$.

7. DISCUSSION AND CONCLUSIONS

The stability of the inverted hexagonal phase depends on energy balance between different contributions to the system free energy, hence the main problem in theoretical description of the lamellar to inverted hexagonal phase transition and explanation of the stability of the H_{II} lipid phase consists in finding the proper expression for the free energy of the system. Most of contemporary theoretical models of the free energy of the inverted hexagonal phase have shown that in addition to the bending energy term, it is necessary to consider also the energy term, which depends on the dimension of the “voids” in the hexagonal lattice, the so-called interstitial energy [24, 31]. We followed this assumption and took into account the interstitial energy which in our model is expressed by the stretching energy of phospholipid chains.

In our theoretical analysis we did not take into account the dependence of the chain stretching modulus τ on the temperature [55], which is based on the elasticity of lipid chains. We expect that neglecting the temperature dependency of τ predicts that the slope of the energy dependence of $|H_m|$ is less pronounced (Fig. 13). Another simplification introduced in our theoretical model is the assumption of spherical cross sections of lipid tubes in the H_{II} phase. The nonspherical cross section of lipid tubes would probably lower the stretching energy of phospholipid chains, but would also contribute to higher bending of the monolayer. To include the deviations from sphericity in our computations will be one of our future tasks in theoretical description of stability of nonplanar lipid phases.

In conclusion, our results indicate that the deviatoric bending can explain the stability of the H_{II} phase at higher temperatures. However, for the L_α - H_{II} transition, tuning of the deviatoric bending energy by the isotropic bending energy and the interstitial energy is needed. Models based on the isotropic elasticity described the L_α - H_{II} phase transition by showing that at a certain temperature, the free energy of the system is lowered as it converts from the L_α phase to the H_{II} phase [56]. However, the energy difference was found to be lower than $0.1kT$ [24]. Our results pursue the general conclusions of the previous models; however, the obtained energy difference becomes much larger at elevated temperatures if the average orientational ordering of anisotropic lipid molecules on highly curved surfaces of the H_{II} phase is taken into account (i.e., if anisotropic elasticity of lipid monolayer is considered). This energy difference is sufficient for the stability of a single cylinder within the lamellar stack and therefore supports previously suggested nucleation models, which are based on LDs [28, 34, 57, 58].

In spite of many simplifications introduced in our theoretical description, results of our modeling and simulations are in good agreement with experimental results [28, 34, 59, 60]. Among others we have shown that

with increasing absolute values of intrinsic curvatures of lipid molecules C_{1m} and C_{2m} (which were assumed to increase with increasing temperature), the L_{α} - H_{II} phase transition occurs beyond a certain threshold temperature. Further we could also reproduce realistic structures in good agreement with experimental results. Our results thus show that deviatoric bending plays an important role in the stability of the inverted hexagonal phase and in the L_{α} - H_{II} phase transition. It should be stressed at the end that considering the deviatoric bending of lipid monolayer [15, 21, 29, 45, 46] does not assume lattice-like packing of anisotropic lipids with fixed orientation and fixed position but just takes into account the possibility of decrease of the free energy of lipid monolayer (bilayer) due to average orientations of laterally mobile rotating anisotropic lipids.

ACKNOWLEDGMENTS

This work was supported by the bilateral Slovenian–Austrian and Austrian–Slovenian Grants BI-AT/07-08-022 and W TZ SI22/2007, respectively, bilateral Slovenian–Czech Grant BI-CZ/07-08-006, and the Grants MSM-6840770012, J3-9219-0381-06, and P2-0232-1538.

REFERENCES

- [1] J.M. Seddon, R.H. Templer, Polymorphism of lipid–water systems, in: A.J. Hoff, R. Lipowsky, E. Sackmann (Eds.), *Handbook of Biological Physics: Structure and Dynamics of Membranes—From Cells to Vesicles*, Vol. 1A Elsevier SPC, Amsterdam, Netherlands, 1995.
- [2] D. Chandler, Two faces of water, *Nature* 417 (2002) 491.
- [3] D. Chandler, Interfaces and the driving force of hydrophobic assembly, *Nature* 437 (2005) 640–647.
- [4] V. Luzzati, A. Tardieu, T. Gulik-Krzywicki, E. Rivas, F. Reiss-Husson, Structure of the cubic phases of lipid–water systems, *Nature* 220 (1968) 485–488.
- [5] P.R. Cullis, M.J. Hope, C.P.S. Tilcock, Lipid polymorphism and the roles of lipids in membranes, *Chem. Phys. Lipids* 40 (1986) 127–144.
- [6] V. Luzzati, Biological significance of lipid polymorphism: The cubic phases, *Curr. Opin. Struct. Biol.* 7 (1997) 661–668.
- [7] K. Larsson, F. Tiberg, Periodic minimal surface structures in bicontinuous lipid–water phases and nanoparticles, *Curr. Opin. Colloid Interface Sci.* 9 (2005) 365–369.
- [8] A. Yaghmur, P. Laggner, S. Zhang, M. Rappolt, Tuning curvature and stability of monoolein bilayers by short surfactant-like designer peptides, *PLoS One* 2 (2007) e479.
- [9] G.S. Attard, J.C. Glyde, C.G. Goltner, Liquid crystalline phases as templates for the synthesis of mesoporous silica, *Nature* 378 (1995) 366–368.
- [10] O.G. Mouritsen, *Life—As a Matter of Fat* Springer, Berlin-Heidelberg, 2005.
- [11] J. Israelachvili, *Intermolecular and Surface Forces* Academic Press Limited, London, UK, 1997.
- [12] S. Leikin, M.M. Kozlov, N.L. Fuller, R.P. Rand, Measured effects of diacylglycerol on structural and elastic properties of phospholipid membranes, *Biophys. J.* 71 (1996) 2623–2632.

- [13] L. Mathivet, S. Cribier, P.F. Devaux, Shape change and physical properties of giant phospholipid vesicles prepared in the presence of an AC electric field, *Biophys. J.* 70 (1996) 1112–1121.
- [14] V. Kralj-Iglič, G. Gomišček, J. Majhenc, V. Arrigler, S. Svetina, Myelin-like protrusions of giant phospholipid vesicles prepared by electroformation, *Colloids Surf. A* 181 (2001) 315–318.
- [15] V. Kralj-Iglič, A. Iglič, G. Gomišček, F. Sevšek, V. Arrigler, H. Hägerstrand, Microtubes and nanotubes of a phospholipid bilayer membrane, *J. Phys. A: Math. Gen.* 35 (2002) 1533–1549.
- [16] A. Iglič, H. Hägerstrand, M. Bobrowska-Hägerstrand, V. Arrigler, V. Kralj-Iglič, Possible role of phospholipid nanotubes in directed transport of membrane vesicles, *Phys. Lett. A* 310 (2003) 493–497.
- [17] M. Bobrowska-Hägerstrand, V. Kralj-Iglič, A. Iglič, K. Bialkowska, B. Isomaa, H. Hägerstrand, Torocyte membrane endovesicles induced by octaethyleneglycol dodecylether in human erythrocytes, *Biophys. J.* 77 (1999) 3356–3362.
- [18] M. Fošnaric, M. Nemeč, V. Kralj-Iglič, H. Hägerstrand, M. Schara, A. Iglič, Possible role of anisotropic membrane inclusions in stability of torocyte red blood cell daughter vesicles, *Colloids Surf. B* 26 (2002) 243–253.
- [19] M. Kandušer, M. Fošnaric, M. Šentjurc, V. Kralj-Iglič, H. Hägerstrand, A. Iglič, D. Miklavčič, Effect of surfactant polyoxyethylene glycol (C12E8) on electroporation of cell line DC3F, *Colloids Surf. A* 214 (2003) 205–217.
- [20] M. Fošnaric, V. Kralj-Iglič, K. Bohinc, A. Iglič, S. May, Stabilization of pores in lipid bilayers by anisotropic inclusions, *J. Phys. Chem. B* 107 (2003) 12519–12526.
- [21] V. Kralj-Iglič, B. Babnik, D.R. Gauger, S. May, A. Iglič, Quadrupolar ordering of phospholipid molecules in narrow necks of phospholipid vesicles, *J. Stat. Phys.* 125 (2006) 727–752.
- [22] A. Iglič, V. Kralj-Iglič, Effect of anisotropic properties of membrane constituents on stable shape of membrane bilayer structure, in: H.T. Tien, A. Ottova-Leitmannova (Eds.), *Planar Lipid Bilayers (BLMs) and Their Applications Elsevier SPC*, Amsterdam, Netherlands, 2003, pp. 143–172.
- [23] V. Kralj-Iglič, M. Remškar, A. Iglič, Deviatoric elasticity as a mechanism describing stable shapes of nanotubes, in: A. Riemer (Ed.), *Horizons in World Physics*, Vol. 244, Nova Science Publishers, Hauppauge, NY, 2004, pp. 111–156.
- [24] M.M. Kozlov, S. Leikin, R.P. Rand, Bending, hydration and interstitial energies quantitatively account for the hexagonal–lamellar–hexagonal reentrant phase transition in dioleoylphosphatidylethanolamine, *Biophys. J.* 67 (1994) 1603–1611.
- [25] M. Rappolt, The biologically relevant lipid mesophases as “seen” by X-rays, *Adv. Planar Lipid Bilayer and Liposomes* 5 (2006) 253–283.
- [26] S. Hyde, S. Anderson, K. Larsson, Z. Blum, T. Landth, S. Lidin, B.W. Ninham, *The Language of Shape Elsevier*, Amsterdam, 1997.
- [27] J.M. Corless, M.J. Costello, Paracrystalline inclusions associated with the disk membranes of frog retinal rod outer segments, *Exp. Eye Res.* 32 (1981) 217–228.
- [28] M. Rappolt, A. Hickel, F. Bringezu, K. Lohner, Mechanism of the lamellar/inverse hexagonal phase transition examined by high resolution X-ray diffraction, *Biophys. J.* 84 (2003) 3111–3122.
- [29] T. Mareš, M. Daniel, Š. Perutková, A. Perne, G. Dolinar, A. Iglič, M. Rappolt, V. Kralj-Iglič, Role of phospholipid asymmetry in the stability of inverted hexagonal mesoscopic phases, *J. Phys. Chem. B* 8 (2008) 16575–16584.
- [30] D.P. Siegel, Inverted micellar intermediates and the transitions between lamellar, cubic, and inverted hexagonal lipid phases, *Biophys. J.* 49 (1988) 1155–1170.
- [31] V.S. Malinin, B.R. Lentz, On the analysis of elastic deformation in hexagonal phases, *Biophys. J.* 86 (2004) 3324–3328.

- [32] D.P. Siegel, The modified stalk mechanism of lamellar/inverted phase transitions and its implications for membrane fusion, *Biophys. J.* 76 (1999) 291–313.
- [33] D.C. Turner, S.M. Gruner, X-ray diffraction reconstruction of the inverted hexagonal (H_{II}) phase in lipid–water systems, *Biophys. J.* 31 (1992) 1340–1355.
- [34] M. Rappolt, A. Hodzic, B. Sartori, M. Ollivon, P. Lagner, Conformational and hydration properties during the L_{β} - to L_{α} - and L_{α} - to H_{II} -phase transition in phosphatidylethanolamine, *Chem. Phys. Lipids* 154 (2008) 46–55.
- [35] B. Kachar, T.S. Reese, Evidence for the lipidic nature of tight junction strands, *Nature* 296 (1982) 464–466.
- [36] S.W. Hui, T.P. Stewart, L.T. Boni, The nature of lipidic particles and their roles in polymorphic transitions, *Chem. Phys. Lipids* 33 (1983) 113–116.
- [37] W. Helfrich, Elastic properties of lipid bilayers: Theory and possible experiments, *Z. Naturforsch. C* 28 (1973) 693–703.
- [38] R.P. Rand, N.L. Fuller, S.M. Gruner, V.A. Parsegian, Membrane curvature, lipid segregation, and structural transitions for phospholipids under dual-solvent stress, *Biochemistry* 29 (1990) 76–87.
- [39] D.P. Siegel, Energetics of intermediates in membrane fusion: Comparison of stalk and inverted micellar intermediate mechanisms, *Biophys. J.* 65 (1993) 2124–2140.
- [40] M. Hamm, M.M. Kozlov, Tilt model of inverted amphiphilic mesophases, *Eur. Phys. J. B* 6 (1998) 519–528.
- [41] J.B. Fournier, Nontopological saddle-splay and curvature instabilities from anisotropic membrane inclusions, *Phys. Rev. Lett.* 76 (1996) 4436–4439.
- [42] V. Kralj-Iglić, V. Heinrich, S. Svetina, B. Žekš, Free energy of closed membrane with anisotropic inclusions, *Eur. Phys. J. B* 10 (1999) 5–8.
- [43] L.D. Landau, E.M. Lifshitz, *Theory of Elasticity* Reed Educational and Professional Publishing Ltd., Oxford, UK, 1986.
- [44] P.B. Canham, The minimum energy of bending as a possible explanation of the biconcave shape of the human red blood cell, *J. Theor. Biol.* 26 (1970) 61–81.
- [45] T. Fischer, Bending stiffness of lipid bilayers. 3. Gaussian curvature, *J. Phys. II (France)* 2 (1992) 337–343.
- [46] T. Fischer, Bending stiffness of lipid bilayers. V. Comparison of two formulations, *J. Phys. II (France)* 3 (1993) 1795–1805.
- [47] T.L. Hill, *An Introduction to Statistical Thermodynamics* General Publishing Company, Toronto, Canada, 1986, pp. 209–211.
- [48] S. May, A molecular model for the line tension of lipid membranes, *Eur. Phys. J. E* 3 (2000) 37–44.
- [49] P. Lagner, M. Kriechbaum, G. Rapp, Structural intermediates in phospholipid phase transitions, *J. Appl. Crystal.* 24 (1991) 836–842.
- [50] J.M. Seddon, J. Robins, T. Gulik-Krzywicki, H. Delacroix, Inverse micellar phases of phospholipids and glycolipids, *Phys. Chem. Chem. Phys.* 2 (2000) 4485–4493.
- [51] H. Delacroix, T. Gulik-Krzywicki, M. Seddon, Freeze fracture electron microscopy of lyotropic lipid systems: Quantitative analysis of the inverse micellar cubic phase of space group $Fd3m$ (Q^227), *J. Mol. Biol.* 258 (1996) 88–103.
- [52] M.A. Churchward, T. Rogasevskaia, D.M. Brandman, H. Khosravani, P. Nava, J.K. Atkinson, J.R. Coorsen, Specific lipids supply critical negative spontaneous curvature—An essential component of native Ca^{2+} -triggered membrane fusion, *Biophys. J.* 94 (2008) 3976–3986.
- [53] S. Kirkpatrick, C.D. Gelatt, M.P. Vecchi, Optimization by simulated annealing, *Science, New Series* 220 (1983) 671–680.
- [54] N. Metropolis, A.W. Rosenbluth, M.N. Rosenbluth, A.H. Teller, E.J. Teller, Equations of state calculations by fast computing machines, *Chem. Phys.* 21 (1953) 1087–1092.

- [55] D. Boal, *Mechanics of the Cell* Cambridge University Press, New York, Cambridge, UK, 2002.
- [56] G. Kirk, S.M. Gruner, D.L. Stein, A thermodynamic model of the lamellar to inverse hexagonal phase transition of lipid membrane–water systems, *Biochemistry* 23 (1984) 1093–1102.
- [57] D.P. Siegel, Inverted micellar intermediates and the transitions between lamellar, cubic, and inverted hexagonal lipid phases. II. Implications for membrane–membrane interactions and membrane fusion, *Biophys. J.* 49 (1986) 1171–1183.
- [58] S.J. Marrink, A.E. Mark, Molecular view of hexagonal phase formation in phospholipid membranes, *Biophys. J.* 87 (2004) 3894–3900.
- [59] P.E. Harper, D.A. Mannoock, R.N.A.H. Lewis, R.N. McElhaney, S.M. Gruner, X-ray diffraction structures of some phosphatidylethanolamine lamellar and inverted hexagonal phases, *Biophys. J.* 81 (2001) 2693–2706.
- [60] G.E.S. Toombes, A.C. Finnefrock, M.W. Tate, S.M. Gruner, Determination of L_{α} – H_{II} phase transition temperature for 1,2-dioleoyl-*sn*-glycero-3-phosphatidylethanolamine, *Biophys. J.* 82 (2002) 2504–2510.